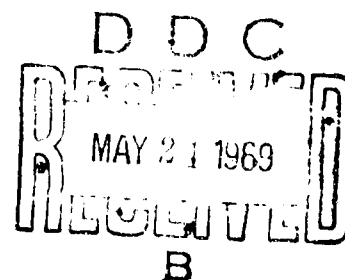ERDE 17/M/68

MINISTRY OF TECHNOLOGY

EXPLOSIVES RESEARCH
AND DEVELOPMENT ESTABLISHMENT

TECHNICAL MEMORANDUM No. 17/M/68

Some Measurements on the Sonic Bangs
Produced at Exercise WESTMINSTER

S.J. Hawkins
J.A. Hicks

AD 68 71 25

WALTHAM ABBEY
ESSEX

38

MINISTRY OF TECHNOLOGY

EXPLOSIVES RESEARCH AND DEVELOPMENT ESTABLISHMENT

TECHNICAL MEMORANDUM No. 17/M/68

Some Measurements on the Sonic Bangs
Produced at Exercise WESTMINSTER

by

S.J. Hawkins and J.A. Hicks

Approved: _E.G. WHITBREAD_
E.G. WHITBREAD
SE

Approved for
Circulation: _____
L.J. BELLAMY
DIRECTOR

2nd October 1968

WALTHAM ABBEY
ESSEX

CONTENTS

1.   SUMMARY

Opportunity was taken at Exercise WESTMINSTER to make recordings of sonic bang waveforms for use as standards of comparison by which the explosively generated simulant waveform under development at ERDE could be judged. A variation of the sonic bang waveform along the aircraft track, first reported in the USA, has been observed in this country for the first time.

From the recorded waveforms, energy spectra and loudness values have been computed, corresponding to the median and extreme forms of the variation. It is concluded that

(i)   the subjective effects of sonic bangs can vary markedly with the location of the observer along the aircraft track, even though the flight conditions and local topography are constant, and

(ii) the ERDE Mark I explosive simulant is very suitable for the assessment of the effects of sonic bangs on building structures.

2.   INTRODUCTION

Exercise WESTMINSTER, held at RAF Upwood, Huntingdonshire on April 21st 1965, had as its main purpose the demonstration of the audible effect of certain types of sonic bang and other noises to a mixed audience comprising Members of Parliament and representatives of Local Government, the Armed Services and Defence Establishments, the Press, Civil Air Lines and other interested organizations.

Apart from this .ain purpose, which invited purely subjective assessments and comparisons by the audience, an obvious opportunity existed of performing measurements of a more scientific nature. The opportunity was a particularly favourable one since a large number of the parameters associated with the generation and propagation of the bangs were to be known, either by predetermination or actual measurement at the time. Thus the aircraft size (type), height, speed and track followed a detailed flight plan which also allowed prediction of the arrival times of the sonic bangs to within a few seconds; stabilized flight was achieved at a point sufficiently distant from 'overhead' that any focussing effects would be attributable solely to atmospheric phenomena; and full meteorological data were available to determine the atmospheric conditions. Furthermore the airfield site offered a large expanse of flat and level open ground where the bangs could be received unmodified by reflections from excrescences such as buildings and trees.

/The .....

The work to be described here fell into this second category and was quite distinct from other work carried out by ERDE in connexion with the main purpose of the exercise (the provision of explosive double bangs for subjective comparison by the audience).

3. BACKGROUND TO THE EXPERIMENT

3.1 General

The determination of the effects of sonic bangs, both in the subjective field of study and in that concerned with structural damage, requires an experimental approach: the physiological and psychological responses of the human and animal organism and the mechanical response of even the simplest building structure being usually dependent upon so many variables known and unknown that useful theoretical work is limited in the one case to statistical processing of experimental data and in the other to approximations based upon simplified models.

Thus a need arises for a large number of sonic bangs to be applied as stimuli or forcings to the experimental system whose response is to be studied, whether this be the population of a city, the cows in a field or the nurseryman's glasshouse.

On the grand scale, where the system to be studied is as large as the above example of the city, then the only practicable method of providing such a large bang field is the direct one of flying supersonic aircraft, as in the American Oklahoma City experiment (1).

To provide a large number of bangs for small scale controlled experiments by this method is impracticable on grounds of both cost and excessive coverage. One is led to seek a method of simulating the sonic bang pressure field over a comparatively small region of space by some cheaper and more easily provided means. This problem was presented to ERDE by Structures Department, RAE Farnborough in late 1963 for investigation of the possibility of a solution using explosives techniques.

3.2 Shape of the Sonic Bang Waveform

The most typical sonic bang waveform in free air near ground level (variations occur) is a symmetrical N-wave (2) with shock amplitudes of the order of a few millibars and having a total duration of the order of 100 - 300 ms (the higher figure refers to projected SST aircraft). Variations commonly found include rounded or spiked extremities of the shocks and minor ripples and perturbations, usually just behind the shock fronts. Occasionally low-amplitude bangs exhibit gross distortion. The amplitude and rise times of the shocks depend upon atmospheric and flight conditions; rise times are commonly in the range 200 μs - 20 ms.

/3.3 .....

- 2 -

3.3 The ERDE Mark I Simulant

The impossibility of using point source explosive charges (i.e. charges whose dimensions are negligible compared with the distance to the point of observation) to simulate the bang waveform is apparent when one compares the time scales involved in typical point source and sonic bang waveforms. To produce a waveform having merely a positive duration of 50 ms – i.e. ignoring all other considerations of shape – would require a charge weighing 136 kg (300 lb) at a distance of 2.13 km (7000 feet).

Investigations in the previously largely unexplored field of linear explosive charges led to a promising technique being devised (3). By a linear charge is meant one whose extension in one dimension (usually along the line-of-sight) is large compared with its other dimensions.

The basic idea leading to this investigation was the realization that an extended charge must give rise to a pressure waveform whose duration – whatever its shape – will be approximately its line-of-sight extension divided by the average shock velocity across that extension. Since for small charges the shock wave decays to within, say, 1% of sonic velocity after only a few metres, it is seen that the average shock velocity across the line-of-sight extension may be closely approximated by sonic velocity and that accordingly a waveform of duration 100 ms, say, will be produced by any charge having a line-of-sight extension of about 34 m (sound speed in air = 340 m/s), the actual shape of the waveform being determined by the distribution of charge along its length.

Theoretical and experimental development of this idea led initially to the derivation of a charge geometry (Mark I) which gave good simulation in most respects of the bang waveform appropriate to a Lightning aircraft. From the pressure/time records obtained the principal apparent defects of the Mark I simulant wave were seen to be firstly the presence of some superimposed random noise and secondly that the stern shock was often of slower rise time than the bow shock. This second defect could be remedied by an additional small point source charge appropriately sited just beyond the distant end of the linear charge, at the expense of some minor aberrations immediately following the stern shock. The first defect presented a more difficult problem since the source of the noise was not known, and its amplitude and frequency distribution varied between otherwise identical firings and also with the terrain over which the firings took place.

/4. .....

- 3 -

4. THE OBJECTS OF THE EXPERIMENT

    4.1 General

        At this juncture it became pertinent to enquire more closely into
    the character of the sonic bang waveform. This was necessary for
    several reasons. Firstly, the general features of the bang waveform as
    described above had been obtained from information supplied by RAE
    Farnborough, but until shortly before Exercise WESTMINSTER no actual
    bang waveforms had been made available for detailed examination. It was
    known from work on transient sounds (4) that one of the most important
    factors determining their loudness is the pressure rise rate: for this
    reason it was important to obtain some measurements indicating the spread
    of rise rates occurring in actual sonic bangs. Secondly, before starting
    any attempt to remove or reduce the residual defects in the simulant it
    was desirable to know to what extent similar alterations appeared in real
    sonic bang waveforms. Thirdly, it had been observed (3) that the sonic
    bang generated by an aircraft in stabilised straight and level flight
    exhibited a marked variation of waveform along the aircraft track. It
    was very desirable to see if this effect – not previously reported out-
    side the USA – could be observed, and to what extent it affected the
    shape of the waveform and hence the range of application of the ERDE
    simulant.

    4.2 Investigation of the Aberrations

        It was clear that the relative importance of defects in the simulant
    wave would depend upon the particular target system envisaged. Thus for
    example in structural damage studies, spurious noise components in the
    middle audio frequency range might well be of no consequence, being well
    above the natural modes of vibration of most structures; whereas in the
    study of the subjective effect upon outdoor personnel such noise
    components could be significant owing to the heavy weighting provided by
    the human ear in this region. A converse situation would apply for sub-
    audio frequencies although low frequency aberrations were in any case
    believed to be small. One aim of the experiment was accordingly to
    obtain the spectral energy distributions of a number of sonic bangs.
    Comparison of these with the distributions obtained from simulant bangs
    would then facilitate decisions as to the suitability of the simulant for
    a particular application. One advantage of working with the spectral
    energy distributions arises in the subjective effects field. Here, an
    important parameter is the loudness: techniques exist for calculating
    this quantity for any type of sound, continuous or transient, from the
    spectral energy distribution, which is therefore a particularly convenient
    form of input datum.

/4.3 .....

- 4 -

4.3 Investigation of the Waveform Variation along the Aircraft Track

It has been reported (1) that a wide variation in waveshape along the aircraft track occurs, even over a distance of the order of a hundred metres, the variation differing for each flight. Definite progressions were noted between highly peaked waves of relatively large overpressure and rounded waves of relatively low overpressure. It has been suggested (5) that these variations resulted from temperature and velocity inhomogeneities in the lower layers of the atmosphere.

A full experimental investigation of the phenomenon would attempt to explore the variation of shape in the ground directions perpendicular to the aircraft track as well as along it. Such an investigation would require a large number of pressure transducers and recording channels; since ERDE equipment totalled only five channels this was out of the question and the aim was accordingly limited to an attempt to confirm the American findings (also with five channels) and to see if the other aberrations were, in fact, constant along the track.

4.4 Instrumentation and Disposition of Gauges

To obtain the spectral energy distribution of the bangs necessitated obtaining pressure/time records with as good a time resolution as could be had, digitizing the waveforms and performing the necessary Fourier analysis and summation into 1/3rd octave bands on an Elliott 503 computer. The resolution of the method of recording (oscilloscope and camera) limited the frequency range to an upper limit of about 500 Hz, this arising since it was necessary to record the whole waveform (of 100 ms duration) along the middle 5 cm of a single 10 cm timebase sweep. High speed data-tape recording would have permitted much better resolution but no equipment of this type was available; however as a check on the occurrence of higher frequencies small portions of the waveforms considered most likely to contain them (i.e. the bow and stern shock fronts) fronts) were recorded simultaneously at ten times the sweep rate, thus permitting measurements up to 5 kHz in these portions.

Quartz piezoelectric transducers of a type known as H3 or B2 by the originating establishments (RARDE and AWRE respectively) and designed for recording blast-wave pressure profiles were used. In these the active crystal faces are mounted flush in the sides of a slim blade-shaped holder which is pointed normally to the incident wavefront. The design of the holder and its support arm, evolved by wind tunnel testing, is fully streamlined; thus the pressure distribution in the recorded wave is minimally affected by reflexions from the support or from the gauge itself, which thus records the true shock profile subject only to a rise-time limitation imposed by the finite diameter of the active faces and the velocity of the shockwave. Since the diameter of the active faces is 2.5 cm, the risetime of the gauges for weak shocks (e.g. sonic bangs) is

/approximately .....

approximately 60 μs. The gauges are highly linear in amplitude response over a wide dynamic range and have a frequency response flat up to just below the lowest resonant mode (approximately critically damped) at about 40 kHz. This bandwidth is not, of course, achieved in practice with weak shocks owing to the above limitation on risetime. In common with all piezoelectric transducers the low frequency half-power point is determined by the time constant of the gauge-plus-electrical load combination. This time constant must be longer than the time occupied by the event to be recorded, by a factor which depends upon the shape of the wave and upon the low frequency distortion which can be tolerated. It is shewn in Appendix II that for an N wave the maximum error in amplitude due to the finite low frequency time constant is of magnitude $P\_/1 - k \ln (1 + k^{-1})\_/$, P being the bow and stern shock amplitudes, and k the ratio of the time gauge constant to τ, where 2τ is the duration of the N-wave. The gauge time constants actually used were approximately 3 seconds, giving a maximum error of about 1% of peak amplitude.

The gauges were coupled to 'straight' d.c. amplifiers having the appropriate input impedance and whose outputs were in turn connected to the Tektronix oscilloscopes used to display the waveforms. Auxiliary triggering microphones were sited upbang from each gauge to enable the oscilloscope timebase sweep to commence slightly before arrival of the wave at the gauge.

The five gauges were disposed on a grassed part of the airfield as shewn in schematic plan in Fig. 1. They were placed close to the ground so that incident and reflected waves were coincident, thus giving well defined N-waves whose amplitudes were equal to the sum of the amplitudes of the incident and reflected waves. Channels 1, 4 and C recorded the whole incident waveform at a sweep rate of 20 ms/cm whilst channels 2 and 3 recorded the stern and bow shocks respectively at a sweep rate of 2 ms/cm and at the same position on the ground as channel C. Thus detailed information was obtainable on the waveform at this position, whilst channels 1, 4 and C, separated by 90 m intervals along the aircraft track, together shewed up any variation of the wave of the type described above.

Channels 1, 2 and 4 were set at a recording sensitivity of 1.2 psf*/cm whilst channel 3 was 0.6 psf/cm and channel C was 0.75 psf/cm. These sensitivites were based on calibrations obtained by RAE Farnborough, for the purposes of this exercise using condenser microphone gauges.

---

*1 psf = 1 lbf/ft^2 ≃ 48 N/m^2

/5. ....

5.   RESULTS AND CONCLUSIONS

The oscilloscope camera records are reproduced as Figs 2 and 3, the events referred to against these are those of the Exercise programme, a copy of which is included in Appendix I. Triggering failures account for the missing records of certain of the events.

The following conclusions may be drawn from the records obtained:

(i) Comparison of the detailed structure of the waves recorded at channels 4, C and 1 for any event shows no similarities in the superimposed ripples and minor perturbations, which must therefore be changing continuously. It would seem reasonable to associate these either with changing propagation conditions due to atmospheric variation along the ray paths of the bang or to the effects of interaction between the incident and ground reflected waves: the detailed structure of the latter might change from point to point over the ground due to inhomogeneities in the surface and hence continuously modify the resultant tant wave at the gauge.

(ii) Comparison of the detailed structure of the bow and stern shocks of any one bang at a given point on the aircraft track almost invariably shews definite similarities. This is what would be expected on either of the hypotheses of (i). Some evidence has been adduced by RAE (5) from measurements made at a height above the ground sufficient to distinguish clearly the incident and reflected waveform, which suggests that the first hypothesis of (i) is the correct one.

(iii) Superficially, the sonic bang waveforms appear to have less random noise than the Mk. I ERDE simulant. We observed a much greater amplitude variation as a result of the peaking and rounding effect described in Section 4.3. The one apparent exception to this was Event Bravo (Fig. 3 (ix), (x)), for which very similar rounded waveforms occurred at all three channels 4, C and 1 along the flight track. Our observations on the variation of waveform are summarised in Fig. 2.

An extrapolated peak pressure, P_e, may be defined in the manner indicated in Fig. 4. This exhibits only small variations along the aircraft track. The "spiked" and "rounded" configurations, however, may differ greatly in peak amplitude, P_m, a ratio of 3 to 1 being observed in Event Golf (Fig. 2b, also Table 1). Table 1 also shows that "spiked" waveforms exhibit shock fronts with the fastest rates of rise of pressure, "rounded" waveforms having the slowest rates.

/TABLE 1 .....

TABLE 1

Event No.	Channel No.	$\overline{P}_e$	P_s	P_m	τ_s	τ_m	RS Ratio	P_s/τ_s
		N/m^2			ms			Nm^{-2}/ms
D1	C	56	33	50	0.30	12	−0.41	100
D1	4	69	46	−	1.3	−	−0.33	35
G1	4	72	72	72	1.4	1.4	0	51
J1	C	81	0	48	−	16	−1.0	−
B2	4	74	91	91	1.2	1.2	+0.23	76
G2	4	63	62	62	2.1	2.1	0	30
J2	4	92	34	62	1.0	8.0	−0.63	34
B3	1	66	43	53	1.5	13	−0.35	29
B3	C	54	33	62	3.4	10	−0.39	9.7
B3	4	79	52	62	2.7	18	−0.34	19
G3	1	58	20	62	0.15	8.0	−0.66	13
G3	C	40	72	72	2.3	2.3	+0.80	31
G3	4	63	182	182	0.80	0.80	+1.9	230
J3	1	87	120	120	1.4	1.4	+0.38	86
J3	C	59	62	81	1.6	5.0	+0.05	39
J3	4	106	55	81	0.90	10	−0.48	61
B4	1	73	110	110	0.47	0.47	+0.51	230
B4	4	86	75	82	1.2	5.0	−0.13	63
D4	1	66	110	110	0.65	0.65	+0.67	170
D4	4	91	52	91	1.5	8.0	−0.43	35
G4	1	60	40	62	0.80	12	−0.33	50
G4	4	69	81	81	1.0	1.0	+0.17	81
J4	1	72	43	63	0.60	5.5	−0.40	72
J4	4	89	75	82	1.7	5.0	−0.16	44

(iv)   The time interval between the bow and stern shocks does not vary significantly throughout the spiked–N–rounded variation of waveform. This also is in accordance with either of the hypotheses of (i).

(v)   The energy spectra of the three distinct types of pressure waveform recorded during overflight Golf on the morning of 21st April, (Figs 2b and 3(iii)) are shewn in Figure 5.   They were obtained by digitizing the experimental records and performing a Fourier analysis and summation into 1/3rd octave bands on an Elliott 503 computer.   In addition, loudness values were calculated by application of Stevens' Mk. 6 procedure (6) to the band-pressure levels, followed by Port's correction for noises of short duration.

/As   .....

As a result of the considerable variations in amplitudes and pressure rise rates of the waveforms along the Event Golf flight path, there is a pronounced variation of the energy spectrum and the loudness value between the spiked (S), N and rounded (R) forms. It is seen from Fig. 5 that for the spiked form there is a very considerable enhancement of the high frequency energy bands over the N and rounded forms. This is reflected also in the loudness values, Table 2.

<div align="center">TABLE 2</div>

Type	P_e	P_m	Loudness Level	Loudness
	N/m²		phon, 1/3rd octave diffuse	sones
R	56	65	103.3	80
N		75	108.3	114
S	62	190	123.3	340

Thus, at an interval of 180 m along the flight track the loudnesses varied over a 4 to 1 ratio. Taking this result as being fairly typical, it is clear that the subjective effects of sonic bangs can vary markedly with the location of the observer, even though the flight conditions and the local topography are constant.

(vi) A comparison of the energy spectra in Fig. 5 for the rounded, N and spiked sonic bang waveforms with that from a 100 ms Mk. I explosive simulant shows that the band energies of the simulant lie everywhere between the limits of variation shown by the real sonic bang. The simulation of the rounded and N waveforms is particularly good in the frequency range up to about 100 Hz.

6. ACKNOWLEDGEMENTS

The authors are indebted to Mr. M.J. Harper for calculations of energy spectra and loudness levels; also to the various members of the ERDE experimental team, who assisted at Exercise WESTMINSTER.

/7. .....

7. ## BIBLIOGRAPHY

1. Hilton, D.A., et al., NASA Technical Note NTD-2539, 1964.

2. Courant, R., and Friedrichs, K.O., "Supersonic Flow and Shock Waves", Interscience, New York, 1948.

3. Hawkins, S.J., and Hicks, J.A., Nature, 1966, 211, 5055, 1244.

4. Zepler, E.E., and Harel, J.R.P., J. Sound Vibr., 1965, 2, 3, 249.

5. Webb, D.R.B., and Warren, C.H.E., Reports and Memoranda No. 3475, HMSO, 1967, (Originally issued as RAE Tech Report No. 65248, 1965.

6. Stevens, S.S., J. acoust. Soc. Am., 1961, 33, 11, 1577.

Specification for Exercise WESTMINSTER

Programme of Events

The following programme of events will take place once in the morning, when it will be experienced out of doors, and once in the afternoon, when it will be experienced indoors. The time of the first event is given as zero (00) and the time of subsequent events is given in minutes after zero.

Event	Time	Description
A	00	Explosive bang at 1 lb/ft^2
B	03	Sonic bang of $1\frac{1}{2}$ lb/ft^2
C	05	Explosive bang of 2 lb/ft^2
D	08	Sonic bang of 2 lb/ft^2
E	12	Flyover by jet aircraft making 110 PNdB
F	15	Explosive bang of $1\frac{1}{2}$ lb/ft^2
G	18	Sonic bang of $1\frac{1}{2}$ lb/ft^2
H	20	Explosive bang of $2\frac{1}{4}$ lb/ft^2
J	23	Sonic bang of $2\frac{1}{4}$ lb/ft^2 (or 2 lb/ft^2 if Event D turns out to be more intense than nominal)
K	27	Flyover by jet aircraft making 110 PNdB
L	30	Explosive bang of $2\frac{1}{4}$ lb/ft^2

The sonic bangs will be made by Lightnings of No. 111 Squadron as follows:-

(a) $1\frac{1}{2}$ lb/ft^2 bangs - M = 1.4, 34,000 ft

(b)   2 lb/ft^2 bangs - M = 1.4, 27,000 ft

(c) $2\frac{1}{4}$ lb/ft^2 bangs - M = 1.4, 25,000 ft.

Distortion of an N-Wave by a High-Pass Filter

The output, $f_{out}(t)$, obtained from a filter of transfer function, $\Phi(p)$, in response to an input, $f_{in}(t)$, is given by:

$$L\left\{f_{out}(t)\right\} = \Phi(p)L\left\{f_{in}(t)\right\} \qquad \cdots\cdots \underline{1}$$

L indicating a Laplace transform. Let the N-wave be parameterized as shewn in Fig. 6, when $f_{in}(t)$ takes the form:

$$f_{in}(t) = \begin{cases} 0 & , \quad 0 > t \\ F\left(1 - \dfrac{t}{\tau}\right), & 0 \leq t \leq 2\tau \\ 0 & , \quad 2\tau < t \end{cases} \qquad \cdots\cdots \underline{2}$$

the transform of which is:

$$L\left\{f_{in}(t)\right\} = F(p) = \int_0^{2\tau} F\left(1 - \frac{t}{\tau}\right) e^{-pt} dt = \frac{P}{p\tau}\left\{e^{-2p\tau}\left(\tau + \frac{1}{p}\right) + \left(\tau - \frac{1}{p}\right)\right\}$$

whilst for a high-pass filter of time-constant T:

$$\Phi(p) = \frac{1}{1 + \dfrac{1}{pT}} \qquad \cdots\cdots \underline{3}$$

Hence, after some manipulation we obtain for $L\{f_{out}(t)\}$:

$$L\left\{f_{out}(t)\right\} = P\left[\frac{T}{\tau} \cdot \frac{1}{p} e^{-2p\tau} + \frac{\tau - T}{\tau} \cdot \frac{1}{p + \dfrac{1}{T}} e^{-2p\tau} + \frac{p - \dfrac{1}{\tau}}{p\left(p + \dfrac{1}{T}\right)}\right] \quad \cdots\cdots \underline{4}$$

Taking inverse transforms and making the substitution

$$T = k\tau \qquad \cdots\cdots \underline{5}$$

/gives .....

gives:

$$f_{out}(t) = \begin{cases} 0 & , \quad 0 > t \\ P\left\{(1 + k)e^{-\frac{t}{T}} - k\right\}, & 0 \leqslant t \leqslant 2\tau \quad \quad \cdots\cdots \; \underline{6} \\ P\left\{(1 - k)e^{\frac{2}{k}} + 1 - k\right\}, & 2\tau < t \end{cases}$$

This is plotted as the dashed line in Fig. 6.

The difference, δ, between the input and the output is thus:

$$\delta = f_{in} - f_{out} = \begin{cases} 0 & , 0 > t \\ P\left\{1 - \frac{t}{\tau} - (1 + k)e^{-\frac{t}{T}} + k\right\}, & 0 \leqslant t \leqslant 2\tau \; \cdots\cdots \; \underline{7} \\ -P\left\{(1 - k)e^{\frac{2}{k}} + 1 + k\right\}e^{-\frac{t}{T}} & , 2\tau < t \end{cases}$$

The maximum value of δ, δ_{max}, is found by equating $\dot{\delta} = 0$

$$\dot{\delta} = P\left\{-\frac{1}{\tau} + \frac{1}{T}(1 + k)e^{-\frac{t}{T}}\right\}, \quad 0 \leqslant t \leqslant 2\tau$$

so that, in this range, $\dot{\delta} = 0$ when $t_{\delta max,} = T \ln\left(1 + \frac{1}{k}\right)$

and the maximum error, δ_{max}, is $P\left\{1 - k \ln\left(1 + \frac{1}{k}\right)\right\}$.

Values of δ_{max} and of $t_{\delta max}$ for various values of k are shewn in Table 1.

/k .....

- 13 -

k	δ_{max}	$t_{\delta max}$
1	.307 P	.693 τ
3	.137 P	.863 τ
10	.047 P	.953 τ
50	.010 P	.980 τ
100	.005 P	.995 τ
∞	0	τ

For example, to obtain a maximum error not greater than 1 per cent of the peak amplitude, the minimum overall low-frequency system time-constant required, when recording 100 ms N-waves, is 2.5 s.

N

90 m

90 m

③

Ⓒ

②

④

HUT HOUSING
RECORDING EQUIPMENT

①

RUNWAY

AIRCRAFT
TRACK
207°

PART OF AIRFIELD
RAF UPWOOD, HUNTS.
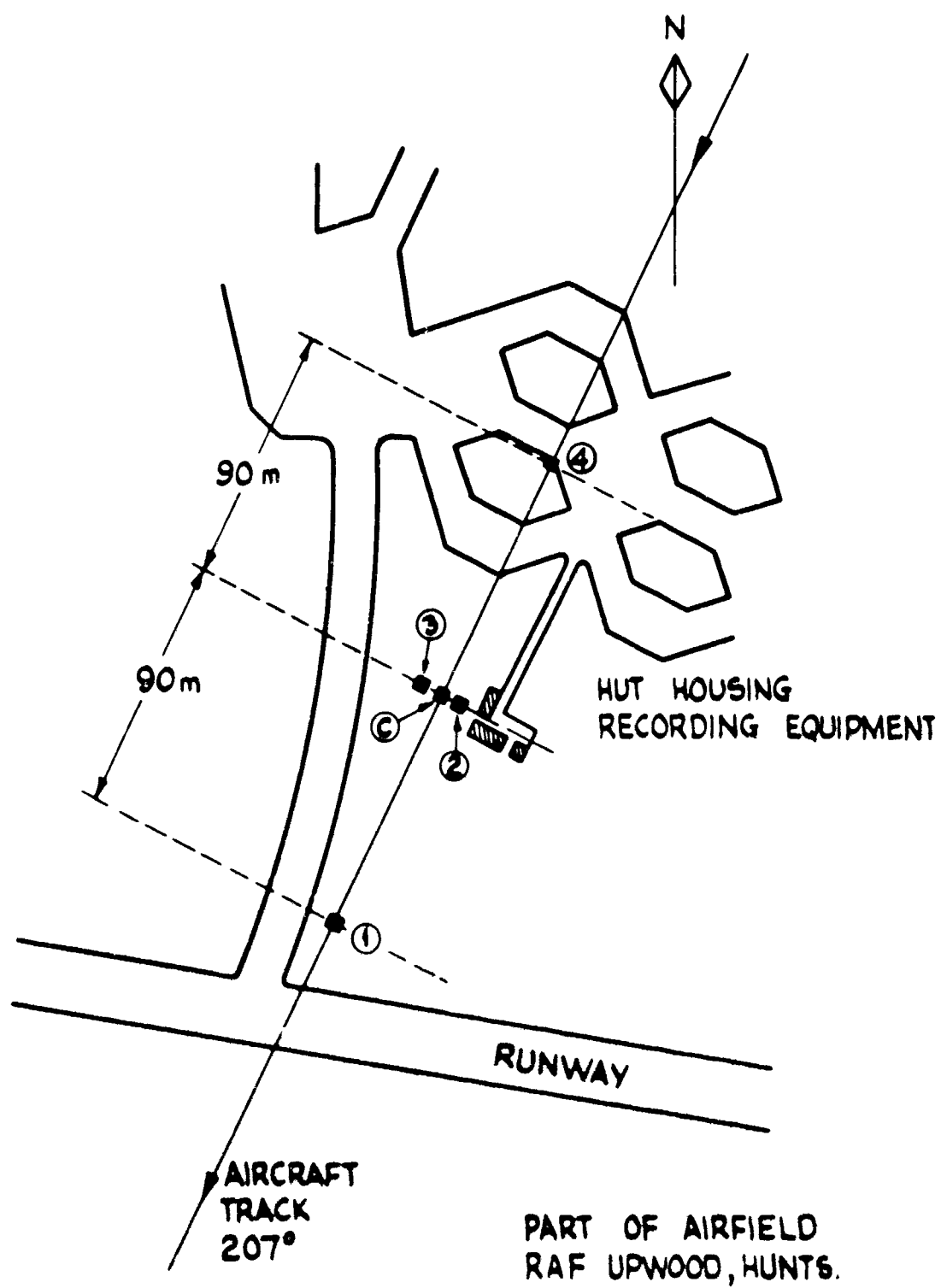
FIG.1   DISPOSITION OF GAUGES ALONG
AIRCRAFT TRACK.

FIG. 2a
EVENT BRAVO
a.m. 21st APRIL.

0.35 R

0.40 R

0.38 R

1.1 psf

1.3 psf

1.3 psf

90 m

80 m

9 000 m-1.4
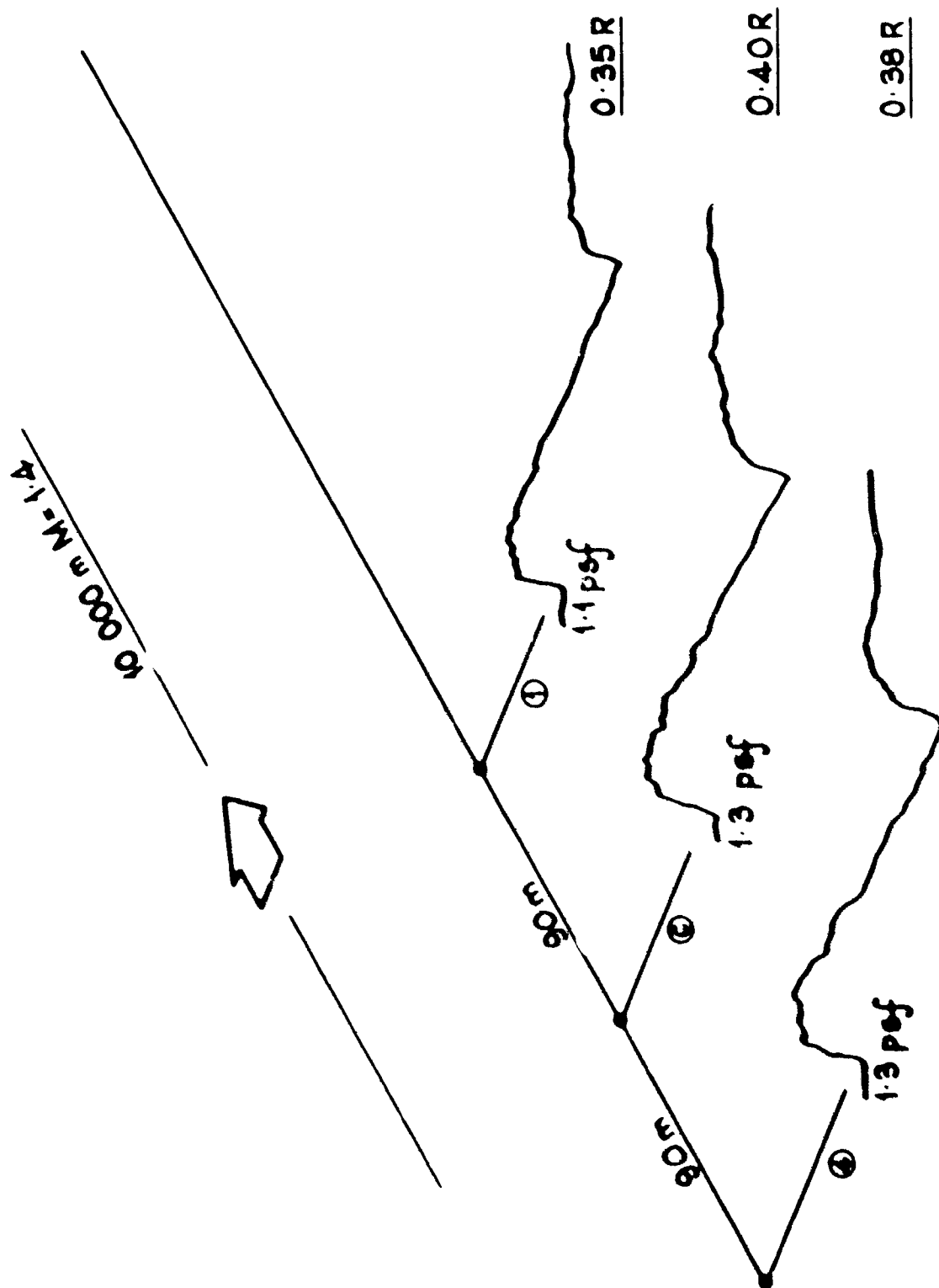
ERDE 17/M/68

FIG. 2b
EVENT GOLF
a.m. 21st APRIL.
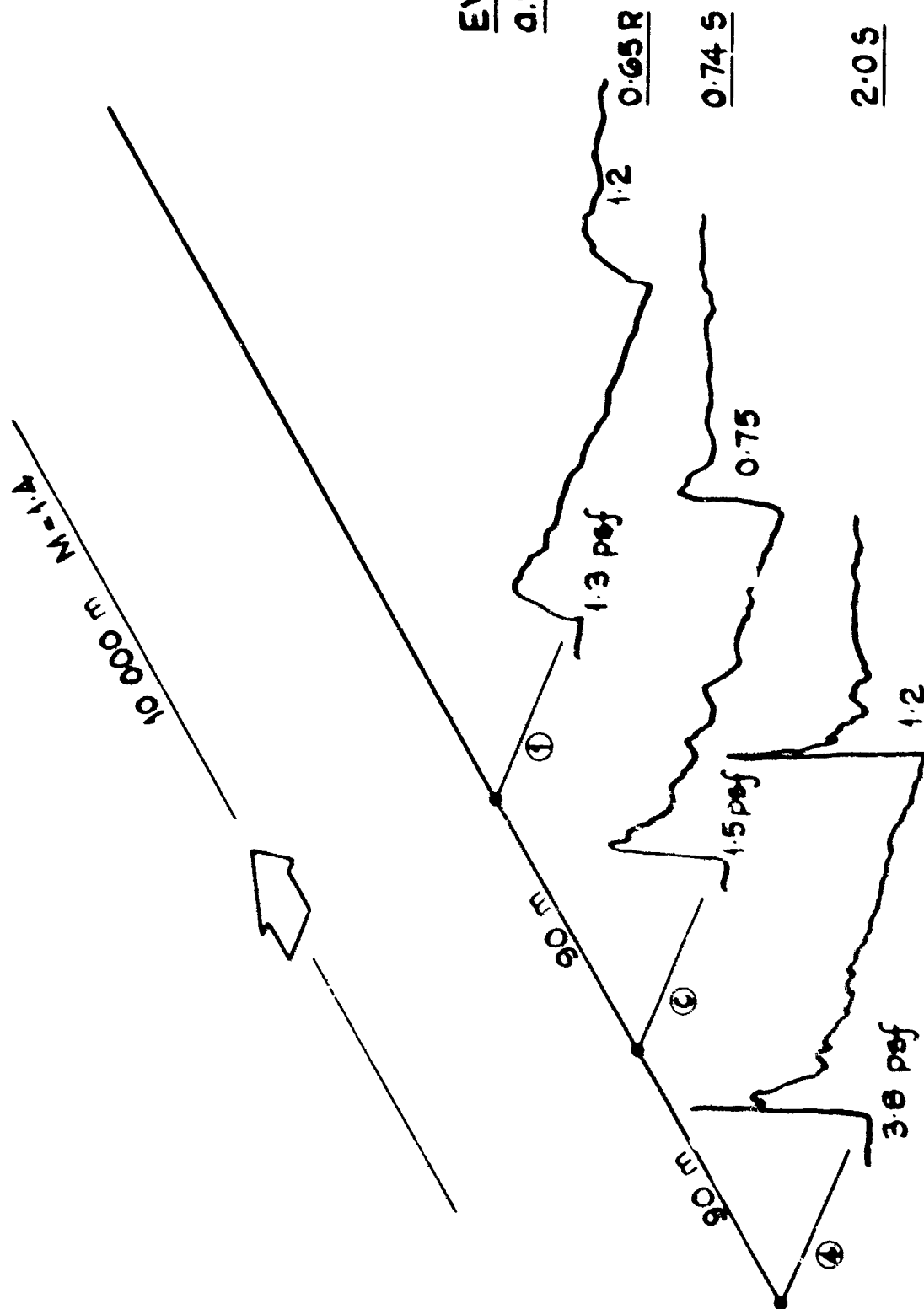
ERDE 17/M/68

FIG. 2c
EVENT JULIET
a.m. 21st APRIL

0·17S

N

0·47 R

8 000 m M=1·4

90 m

2·5 psf

1·7 psf

1·7 psf

90 m
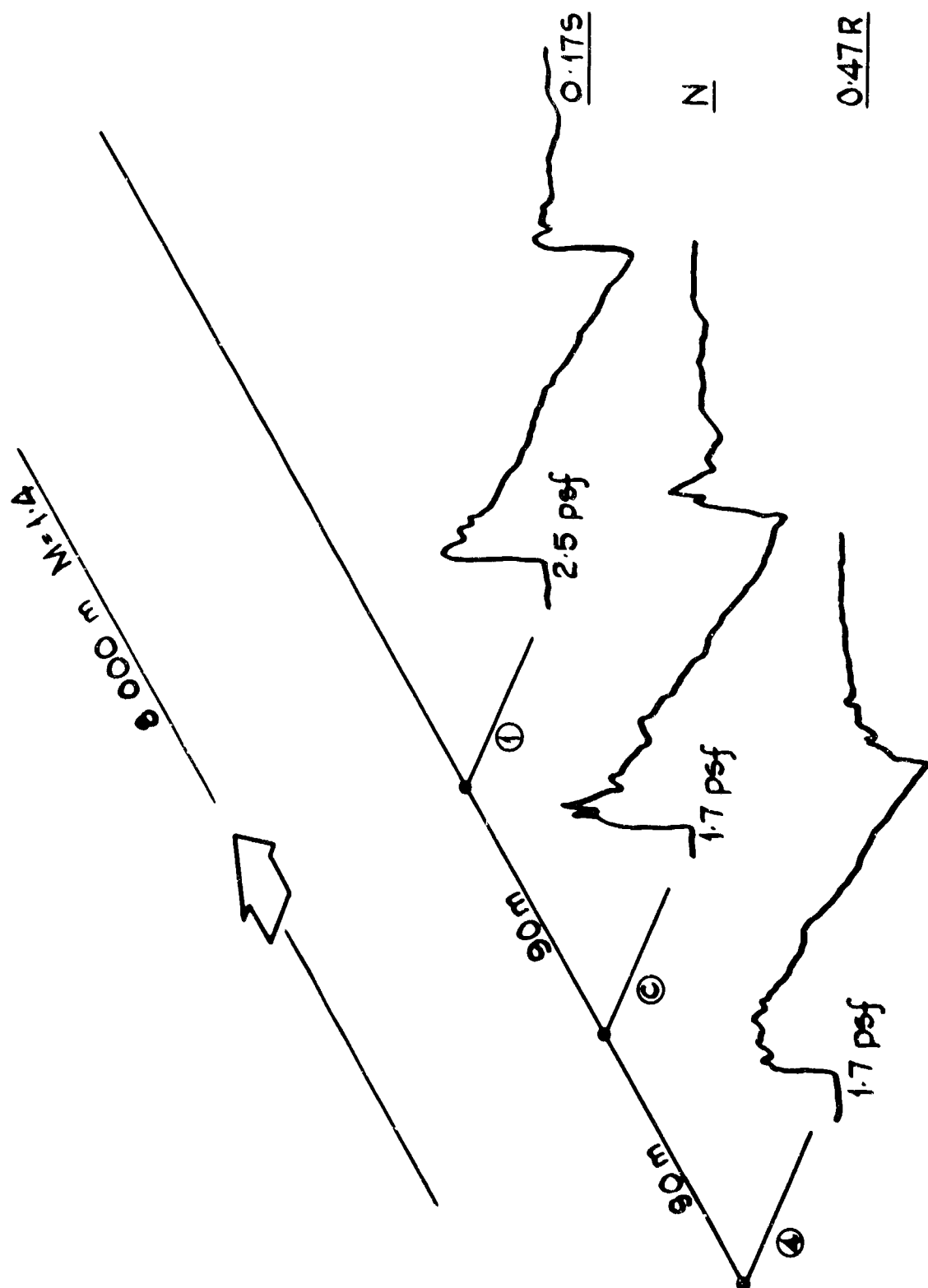
ERDE 17/M/68

FIG. 2d
EVENT BRAVO
p.m. 21st APRIL.

0·33 s

0·13 R

2·3 psf

10 000 m   M=1·4

①

(N WAVE)

90 m

1·7 psf

90 m

④
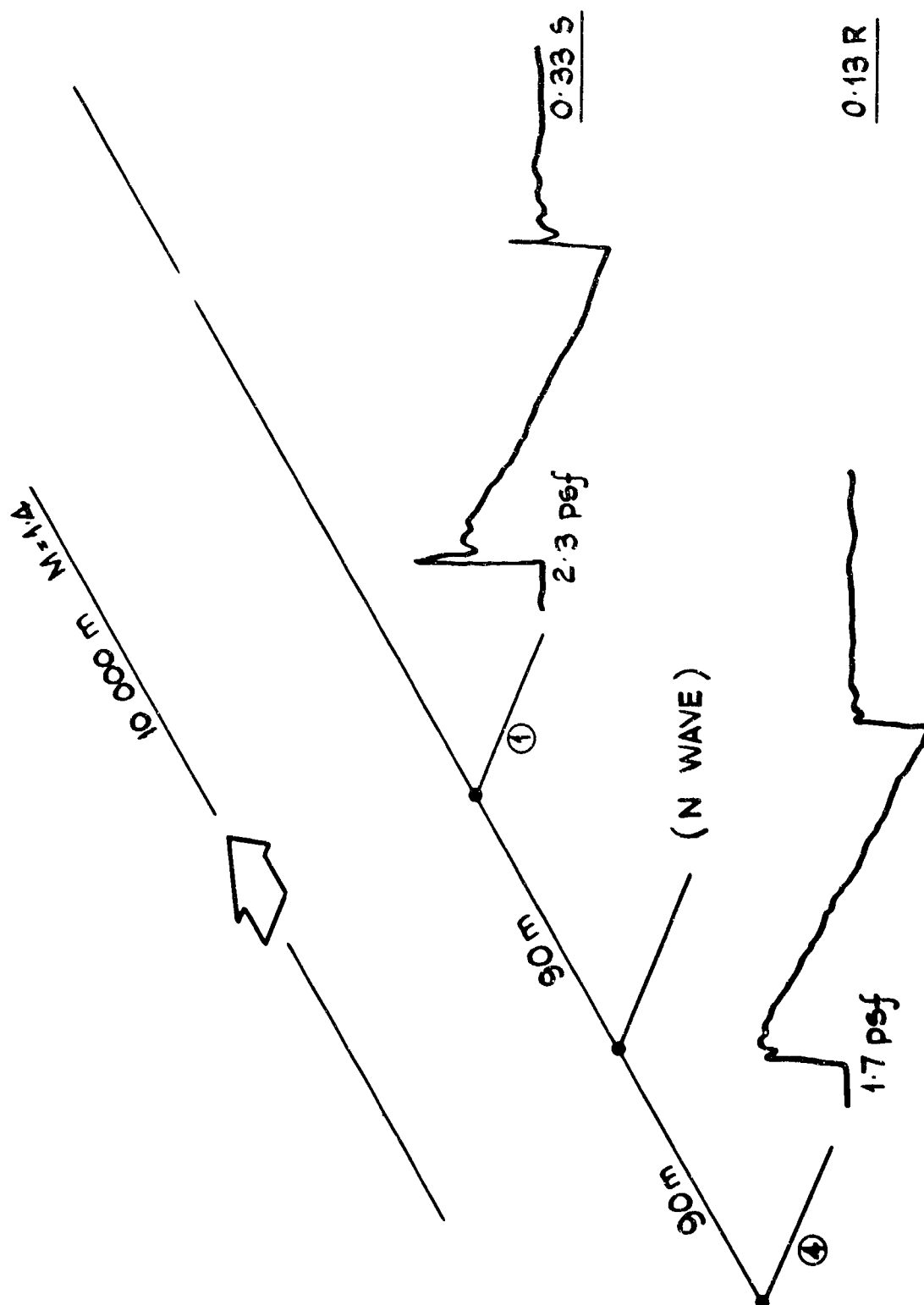
ERDE 17/M/68

FIG. 2c
EVENT DELTA
p.m. 21st APRIL.
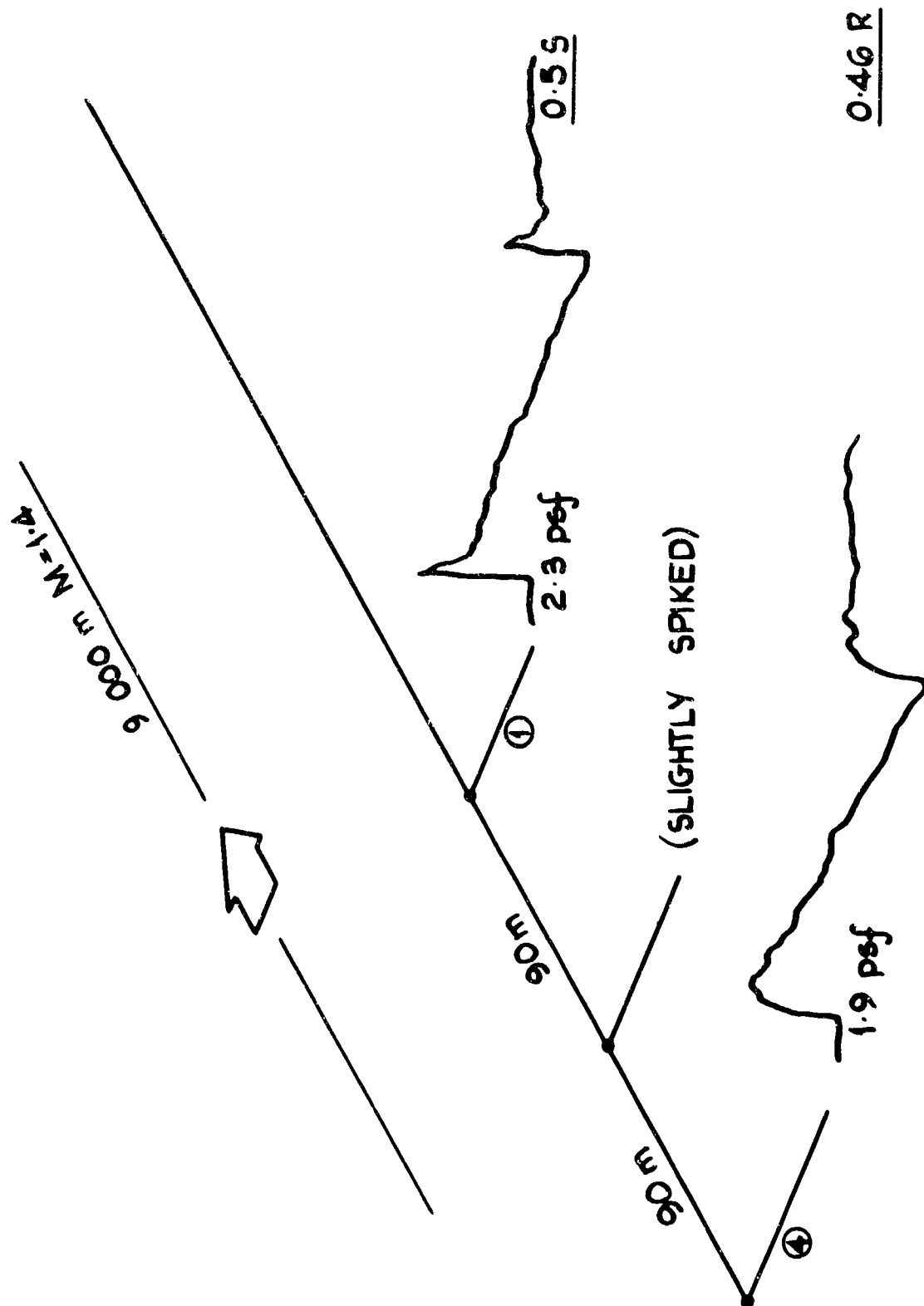
ERDE 17/M/68

FIG. 2f
EVENT GOLF
p.m. 21st APRIL.
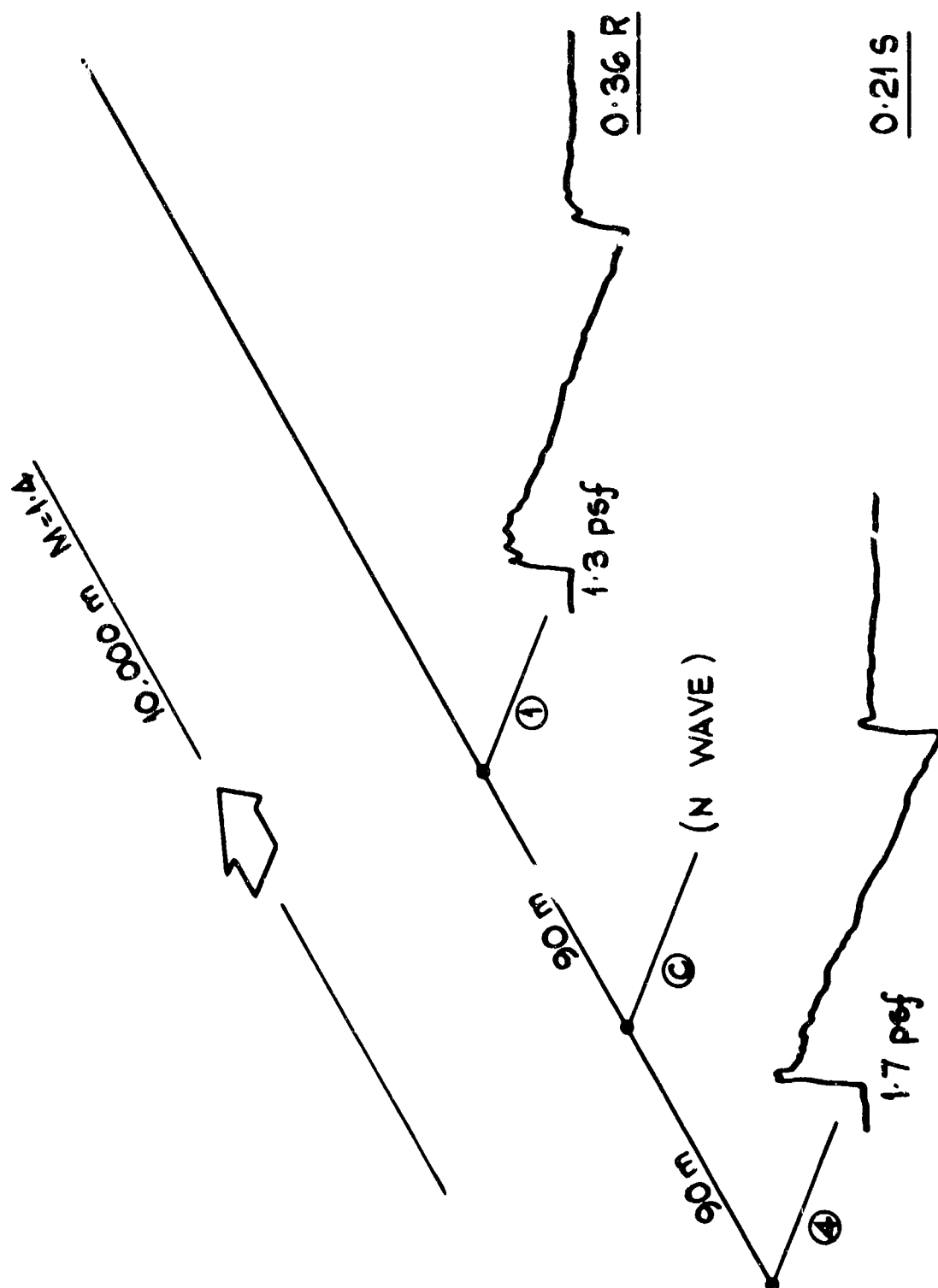
Pressures in parentheses are valves reported by RAE, the measurements being made at a point approximately 400 m from the ERDE gauges in a direction roughly 45° to the aircraft track.

1 psf $\approx$ 48 N/m^2

ERDE 17/M/68
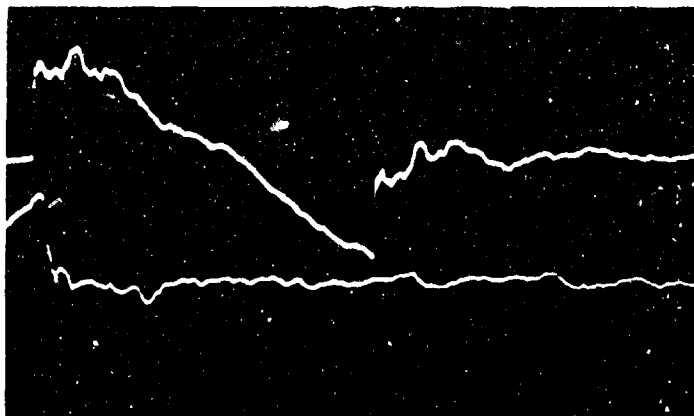
Fig. 3(i)

Event Delta   a.m. 20th April

CHANNELS C (Upper)
         4 (Lower)

TB: 20 ms/cm
Sensitivity: C, 0.75 psf/cm
              4, 1.2 psf/cm
Peak Pressure: C, 1.0 psf (1.9)
               4, -
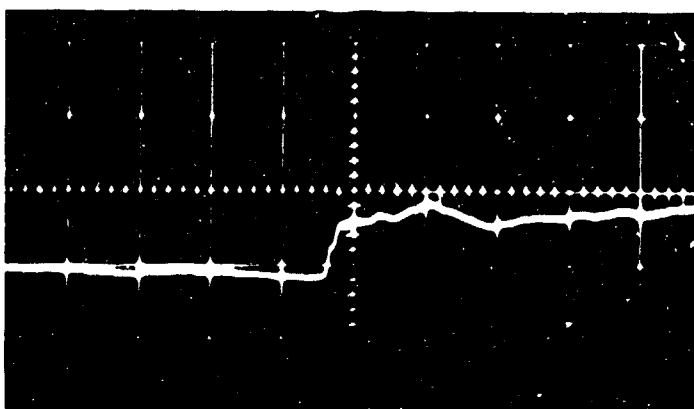
Fig. 3(ii)

Event Delta   a.m. 20th April

CHANNEL 2

TB: 2 ms/cm
Sensitivity: 1.2 psf/cm

Stern Shock
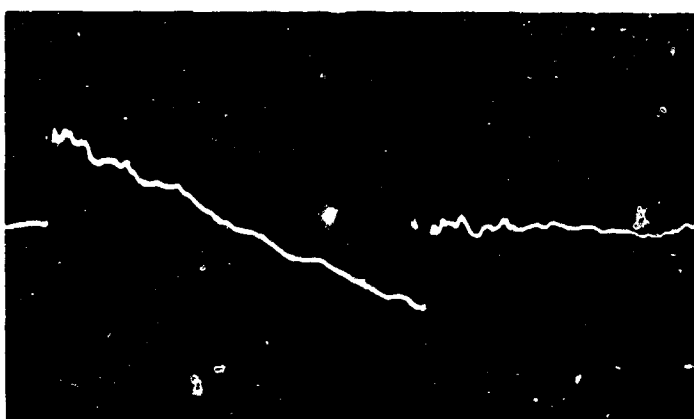
Fig. 3(iii)

Event Golf   a.m. 20th April

CHANNEL 4

TB: 20 ms/cm
Sensitivity: 1.2 psf/cm
Peak Pressure: 1.6 psf (1.0)
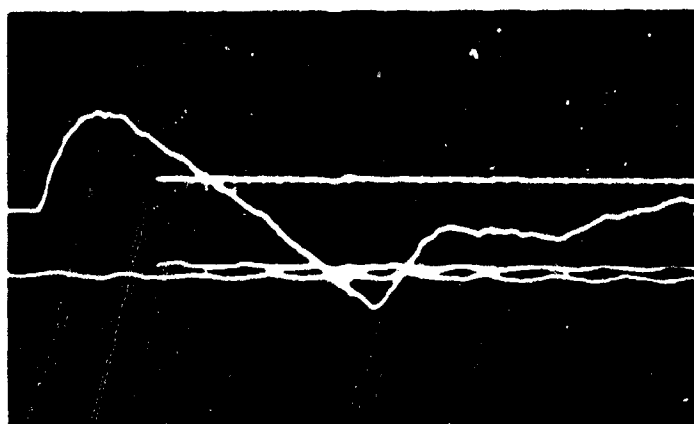
Fig. 3(iv)

Event Juliet   a.m. 20th April

CHANNEL C

TB: 20 ms/cm
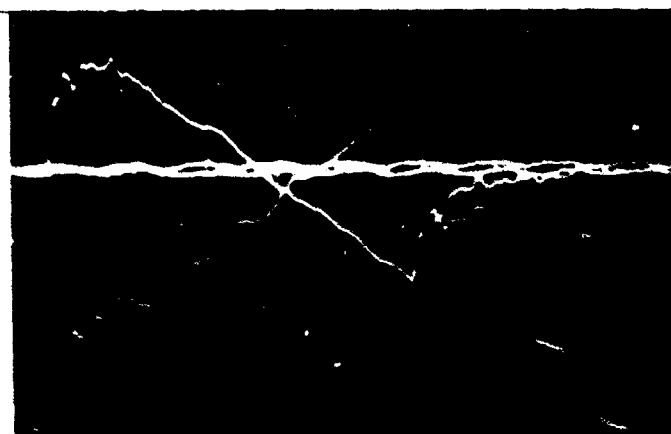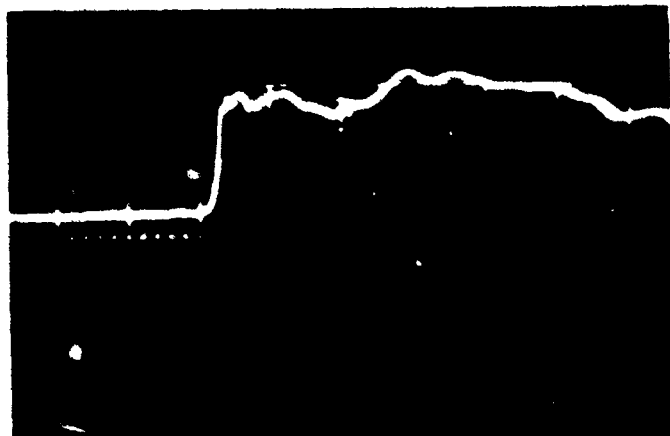Sensitivity: 0.75 psf/cm
Peak Pressure: 1.0 psf (1.8)
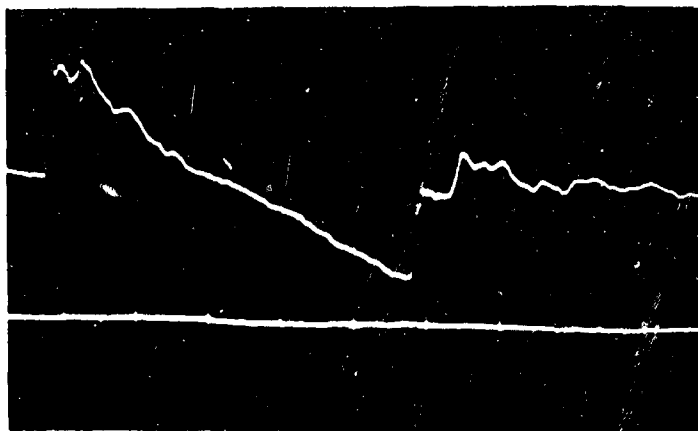
Fig. 3(v)

Event Bravo   p.m. 20th April

CHANNEL 4

TB: 20 ma/cm
Sensitivity: 1.2 psf/cm
Peak Pressure: 2.0 psf (-)
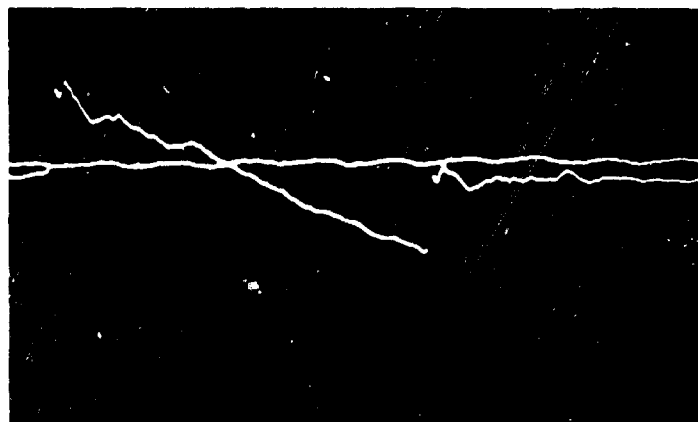
Fig. 3(vi)

Event Golf   p.m. 20th April

CHANNEL 4

TB: 20 ma/cm
Sensitivity: 1.2 psf/cm
Peak Pressure: 1.5 psf (-)
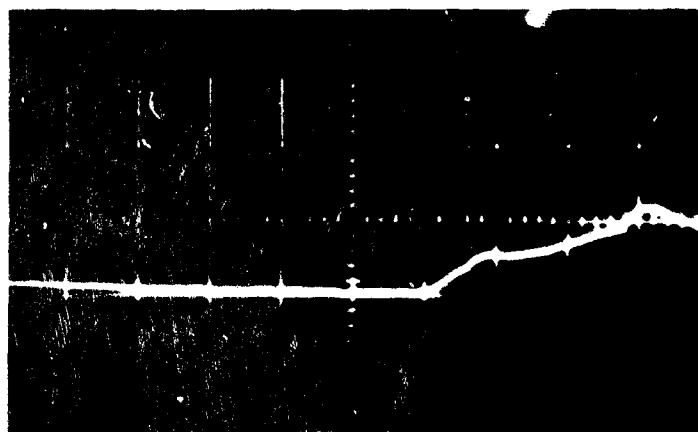
Fig. 3(vii)

Event Golf   p.m. 20th April

CHANNEL 2

TB: 2 ma/cm
Sensitivity: 1.2 psf/cm

Stern Shock
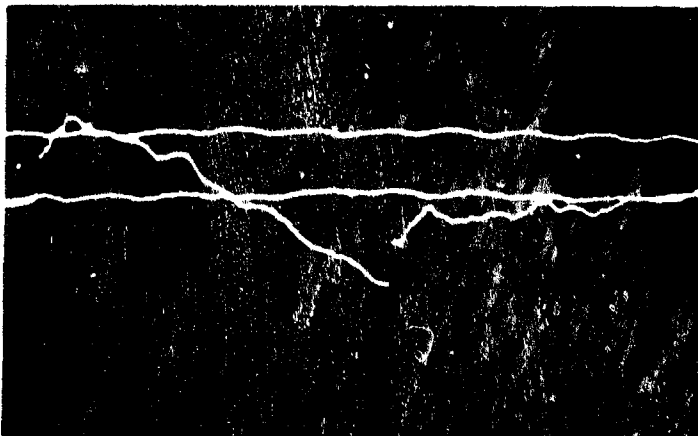
Fig. 3(viii)

Event Juliet p.m. 20th April

CHANNEL 4

TB: 20 ma/cm
Sensitivity: 1.2 psf/cm
Peak Pressure: 1.5 psf (-)
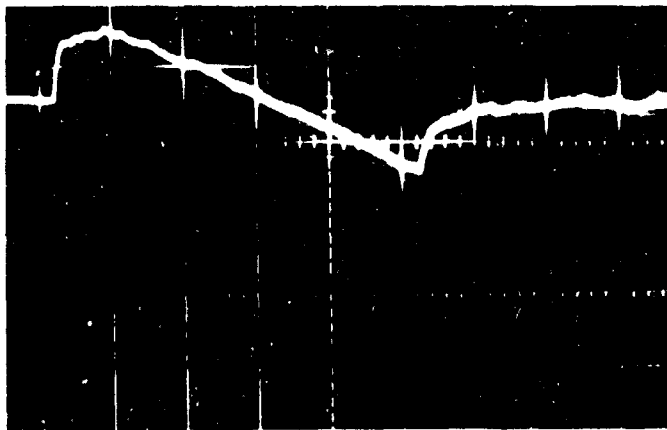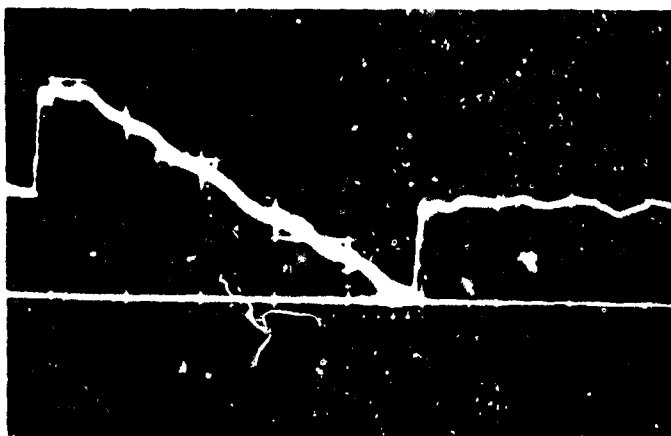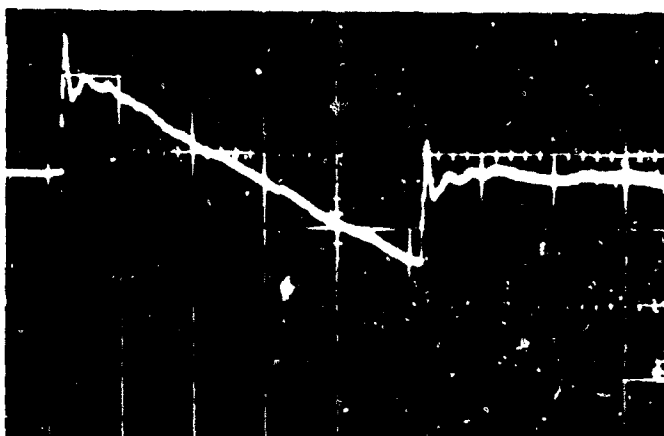
Fig. 3(ix)

Event Bravo   a.m. 21st April

CHANNEL 1

TB: 20 ms/cm
Sensitivity: 1.2 psf/cm
Peak Pressure: 1.1 psf (2.2)

Fig. 3(x)

Event Bravo   a.m. 21st April

CHANNELS 4 (Upper)
         C (Lower)

TB: 20 ms/cm
Sensitivities: 4, 1.2 psf/cm
                C, 0.75 psf/cm
Peak Pressures: 4, 1.3 psf (2.2)
                C, 1.3 psf
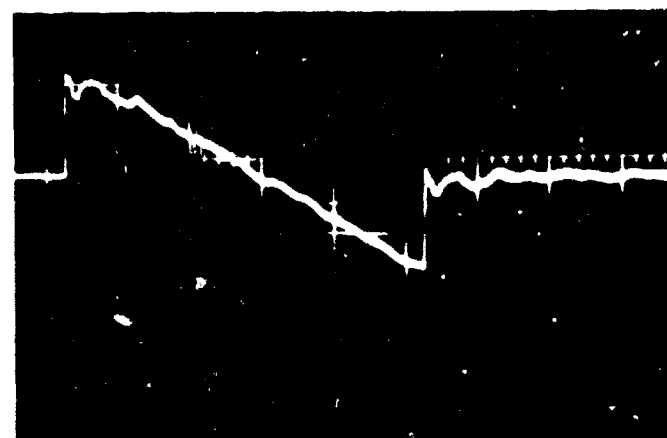
Fig. 3(xi)

Event Delta   a.m. 21st April

CHANNEL 1

TB: 20 ms/cm
Sensitivity: 1.2 psf/cm
Peak Pressure: 1.7 :sf (2.0)
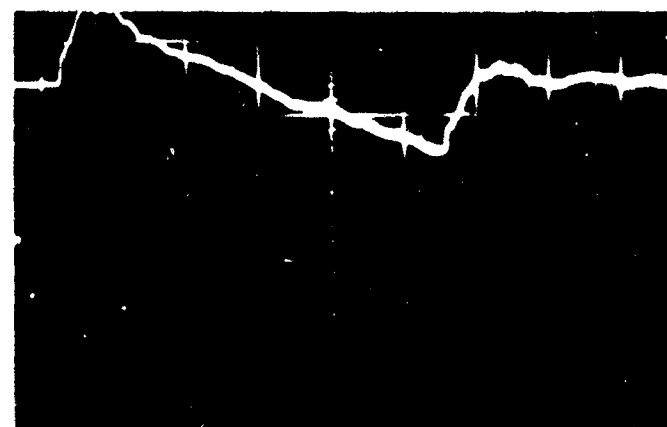
Fig. 3(xii)

Event Golf   a.m. 21st April

CHANNEL 1

TB: 20 ms/cm
Sensitivity: 1.2 psf/cm
Peak Pressure: est.1.3 psf (1.0)
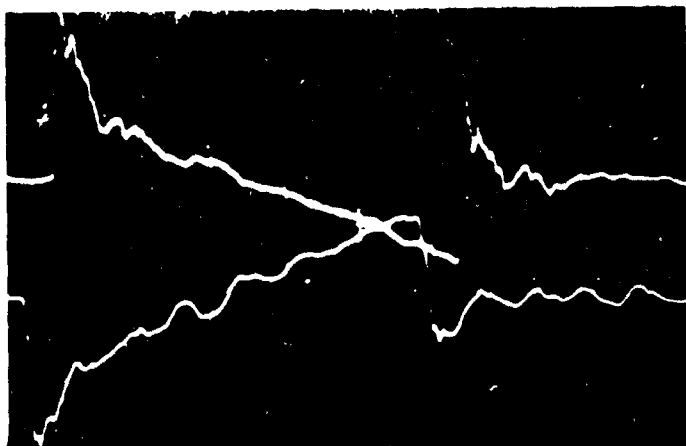
Fig. 3(xiii)

Event Golf   a.m. 21st April

CHANNELS 4 (Upper)
         C (Lower)

TB: 20 ms/cm
Sensitivities: 4, 1.2 psf/cm
                C, 0.75 psf/cm
Peak Pressures: 4, over 3.6 psf
                       (1.0)
   C, 1.5 psf
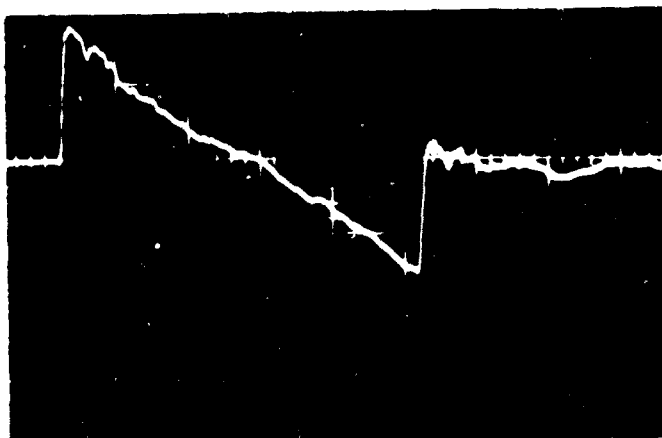
Fig. 3(xiv)

Event Juliet   a.m. 21st April

CHANNEL 1

TB: 20 ms/cm
Sensitivity: 1.2 psf/cm
Peak Pressure: 2.5 psf (1.9)

Fig. 3(xv)

Event Juliet   a.m. 21st April

CHANNELS 4 (Upper)
         C (Lower)

TB: 20 ms/cm
Sensitivities: 4, 1.2 psf/cm
                C, 0.75 psf/cm
Peak Pressures: 4, 1.7 psf (1.9)
                C, 1.7 psf

Fig. 3(xvi)

Event Juliet   a.m. 21st April

CHANNEL 3

TB: 2 ms/cm
Sensitivity: 0.6 psf/cm
Peak Pressure: 1.0 psf (1.9)

Bow Shock

ERDE 17/M/68
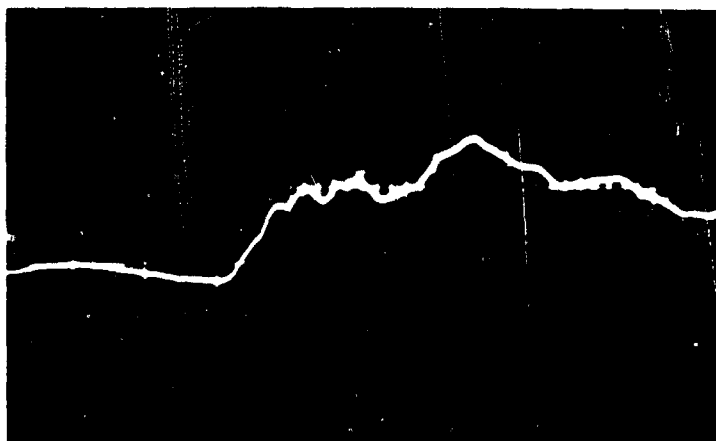
Fig. 3(xvii)

Event Juliet   a.m. 21st April

CHANNEL 2

TB: 2 ma/cm
Sensitivity: 1.2 psf/cm

Stern Shock

ERDE 17/M/68

Fig. 3(xviii)

Event Bravo   p.m. 21st April

CHANNEL 4

TB: 20 ms/cm
Sensitivity: 1.2 psf/cm
Peak Pressure: 1.7 psf (1.3)

Fig. 3(xix)

Event Bravo   p.m. 21st April

CHANNEL 1

TB.   20 ms/cm
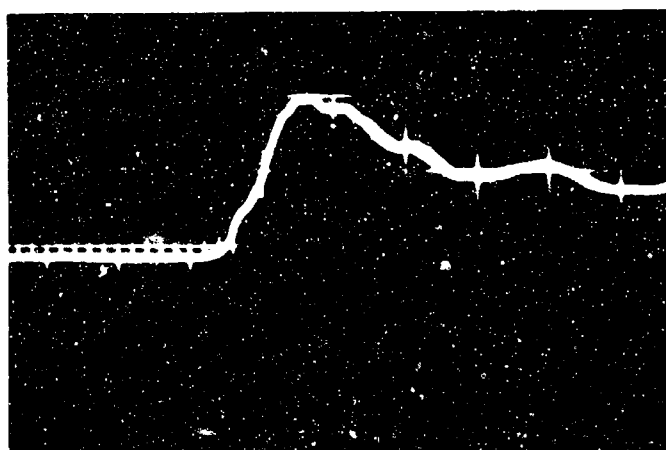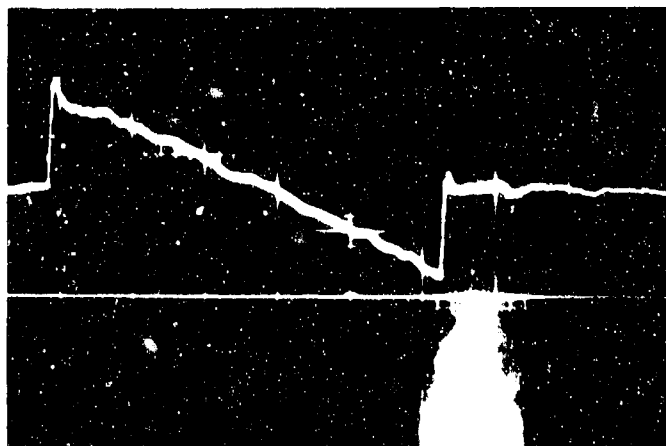Sensitivity: 1.2 psf/cm
Peak Pressure: 2.3 psf (1.3)
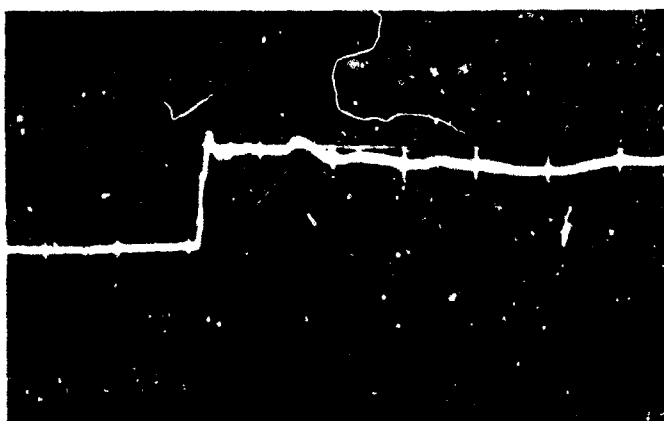
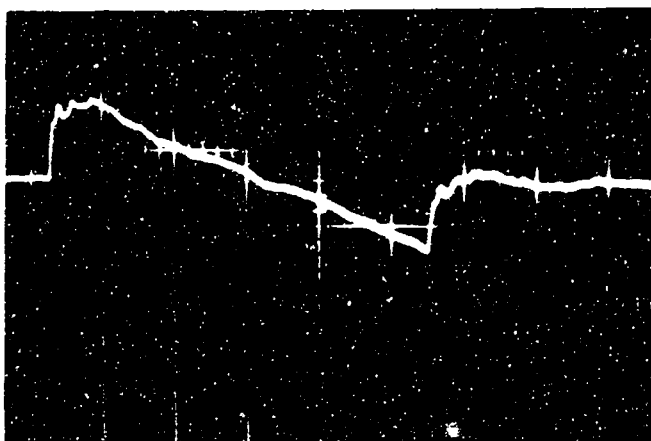Fig. 3(xx)

Event Bravo   p.m. 21st April

CHANNEL 3

TB: 2 ms/cm
Sensitivity: 0.6 psf/cm
Peak Pressure: 1.0 psf (1.3)
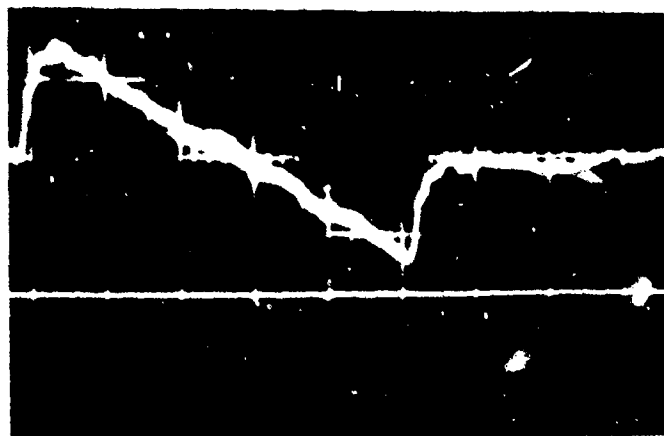
Fig. 3(xxi)

Event Delta   p.m. 21st April

CHANNEL 4

TB: 20 ms/cm
Sensitivity: 1.2 psf/cm
Peak Pressure: 1.9 psf (1.3)

ERDE 17/M/68
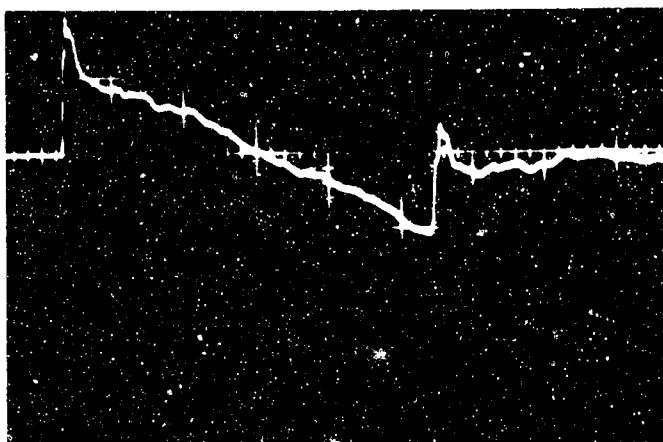
Fig. 3(xxii)

Event Delta   p.m. 21st April

CHANNEL 1

TB: 20 ms/cm
Sensitivity: 1.2 psf/cm
Peak Pressure: 2.3 psf (1.3)

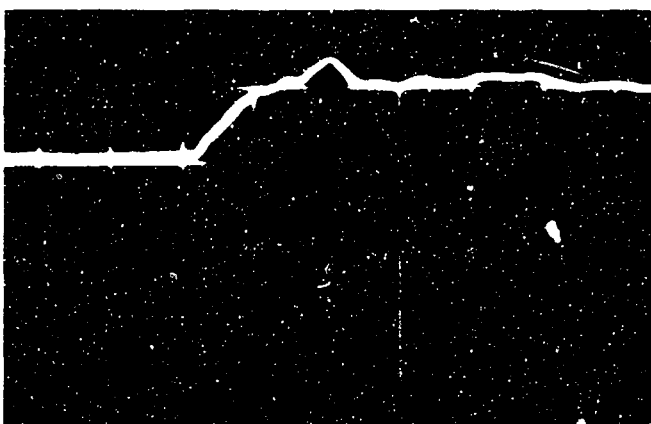Fig. 3(xxiii)

Event Delta   p.m. 21st April

CHANNEL 3

TB: 2 ms/cm
Sensitivity: 0.6 psf/cm
Peak Pressure: 1.3 psf (1.3)

Leading Edge
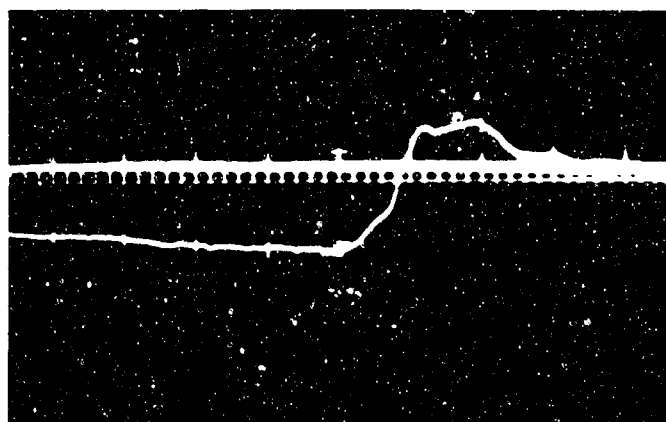
Fig. 3(xxiv)

Event Delta   p.m. 21st April

CHANNEL 2

TB: 2 ms/cm
Sensitivity: 1.2 psf/cm

Trailing Edge

Fig. 3(xxv)

Event Golf   p.m. 21st April

CHANNEL 4

TB: 20 ms/cm
Sensitivity: 1.2 psf/cm
Peak Pressure: 1.7 psf (1.3)

ERDE 17/M/68

Fig. 3(xxvi)

Event Golf   p.m. 21st April

CHANNEL 1

TB: 20 ms/cm
Sensitivity: 1.2 psf/cm
Peak Pressure: 1.3 psf (1.3)

Fig. 3(xxvii)

Event Golf   p.m. 21st April

CHANNEL 3

TB: 2 ms/cm
Sensitivity: 0.6 psf/cm
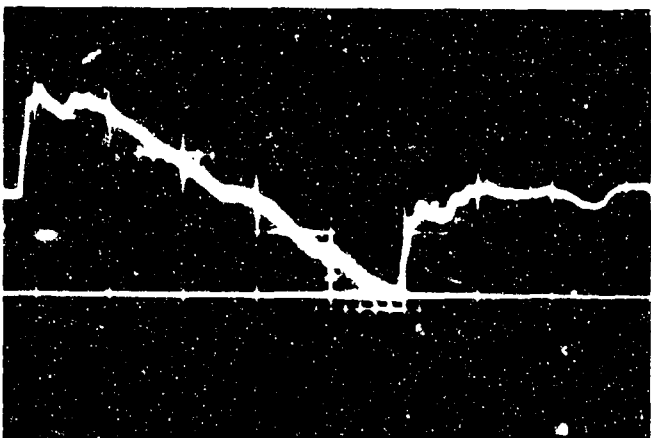Peak Pressure: 0.8 psf (1.3)

Leading Edge

Fig. 3(xxviii)

Event Juliet   p.m. 21st April

CHANNEL 4

TB: 20 ms/cm
Sensitivity: 1.2 psf/cm
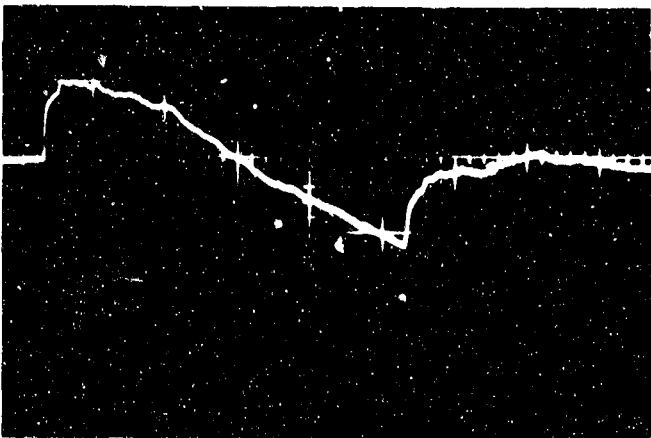Peak Pressure: 1.7 psf (1.3)

Fig. 3(xxix)

Event Juliet   p.m. 21st April

CHANNEL 1

TB: 20 ms/cm
Sensitivity: 1.2 psf/cm
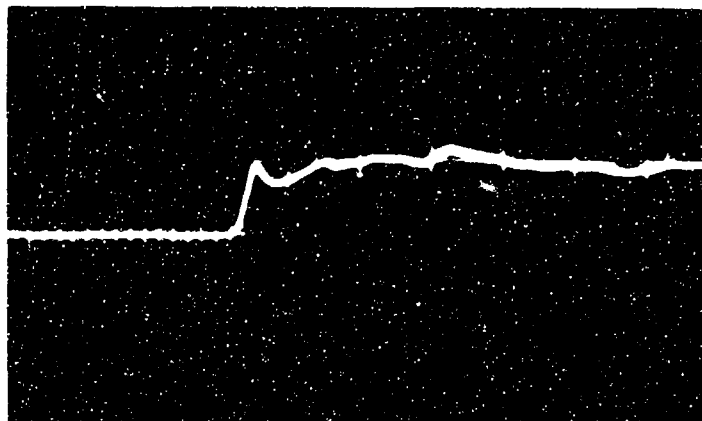Peak Pressure: 1.3 psf (1.3)

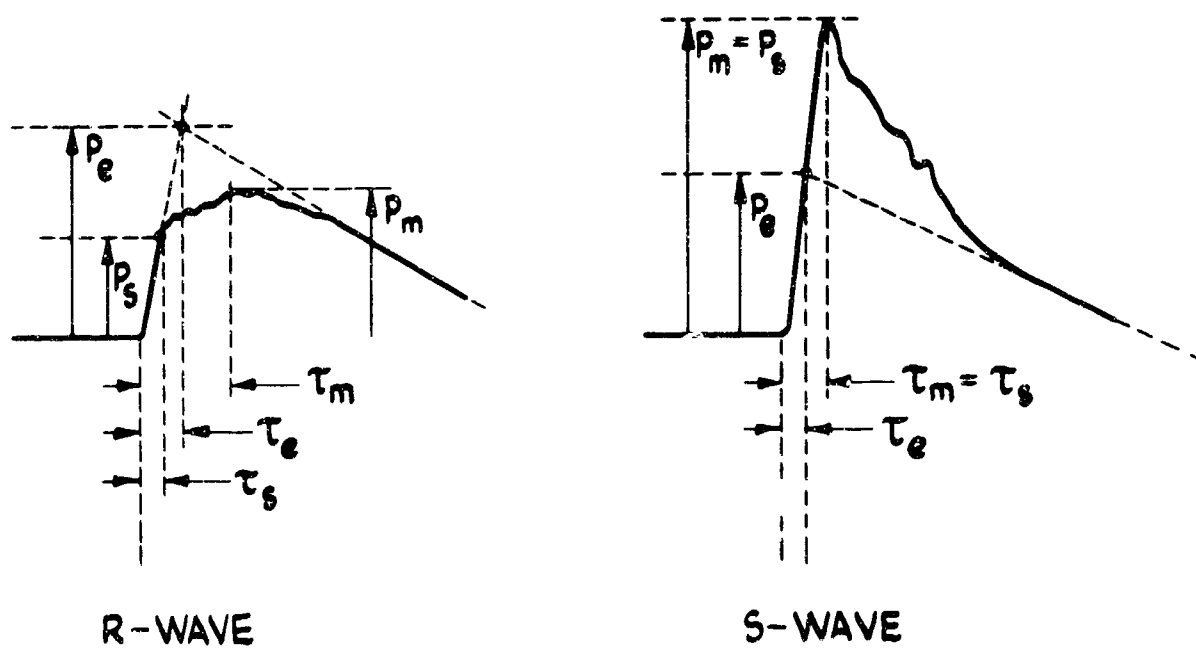# ERDE 17/M/68

Fig. 3(xxx)

Event Juliet   p.m. 21st April

CHANNEL 3

TB: 2 ms/cm
Sensitivity: 0.6 psf/cm
Peak Pressure: 0.6 psf (1.3)

Leading Edge

R-WAVE

S-WAVE

$$RS \text{ Ratio} = \frac{P_s - P_e}{P_e}$$

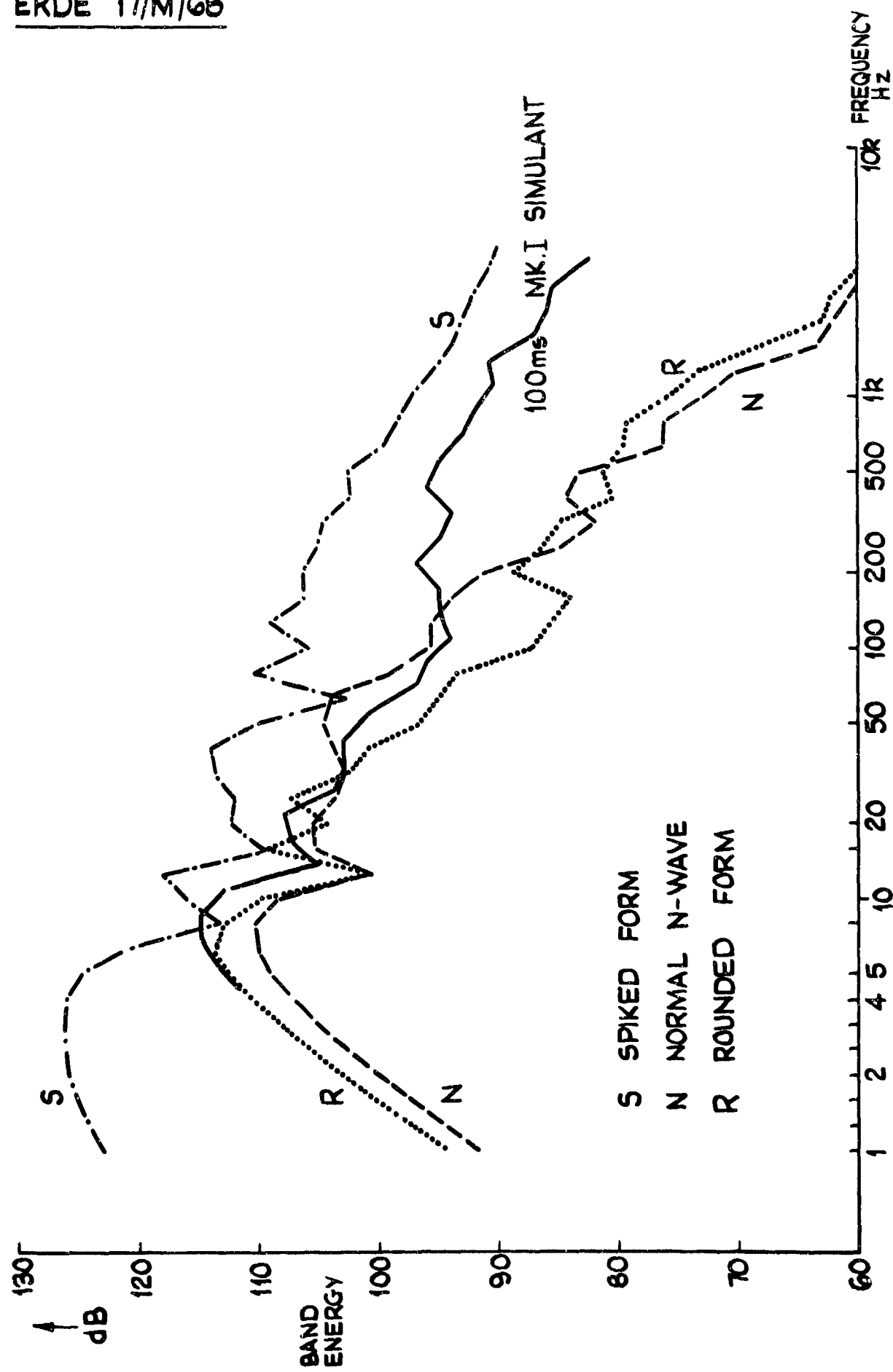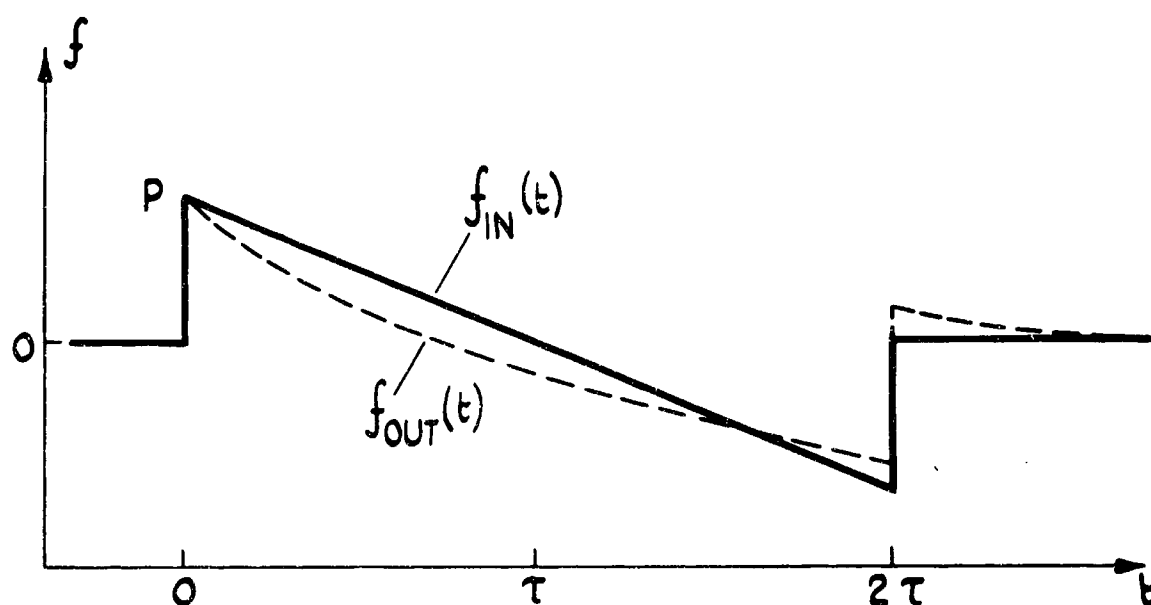FIG. 4   PARAMETERIZATION OF S- AND R-WAVEFORMS.

FIG.5   SONIC BANGS FROM 'LIGHTNING' AIRCRAFT.

$$
f_{OUT}(t) = \begin{cases} P\left[(1+K)e^{-t/T} - K\right] & , \ 0 \leqslant t \leqslant 2\tau \\[2ex] P\left[(1-K)e^{2/K} + 1 + K\right]e^{-t/T} & , \ 2\tau < t \end{cases}
$$

FIG. 6   RESPONSE OF HIGH — PASS FILTER TO N-WAVE.